Journal of Visualization, Vol. 1, No. 3 (1999) 271-281

Vortex Structures and Temperature Fluctuations in a Bluff-body Burner

Nishimura, T.*, Kaga, T.*, Shirotani, K.* and Kadowaki, J.*

* Department of Mechanical Engineering, Yamaguchi University, Ube, 755-8611, Japan.

Received 4 August 1998.
Revised 30 October 1998.

***Abstract*:** Vortical and thermal structures of non-premixed propane flame in a bluff-body burner are studied experimentally in the transition from laminar to turbulent flow. In particular, we focus attention on the effect of annular air flow on the flame. The small-scale inner vortices inside the flame is stimulated by the annular air flow, and outside the flame, small eddies due to turbulence rather than the large-scale outer vortices due to thermal buoyancy become dominant with increasing air velocity. The interrelation between the vortical and thermal structures is analyzed by looking at the frequency spectrum and probability density function of temperature fluctuations.

***Keywords*:** combustion, non-premixed flame, shadowgraph method vortical structure, thermal structure, bluff-body burner

1. Introduction

Non-premixed flame stabilized by a bluff-body combustor, such as occurs when a central fuel jet issues into a surrounding annular air flow, is often used industrially. Such bluff-body combustors provide good flame stabilization as well as easy control of combustion.

There have been experimental studies on non-premixed flames for several fuels. Roquemore et al. (1986) introduced a two-diemsional sheet-lighting technique coupled with a fast chemically reacting system to visualize the turbulent mixing and the vortex shedding processes of a bluff-body combustor for C_3H_8. Lin and Tankin (1987) employed this technique and determined the effect of burner design and flow conditions on fuel jet penetration at low Reynolds numbers. Furthermore, Chin and Tankin (1991) and Nishimura and Takemori (1995) measured vortical shedding frequency using a flow visualization technique in a two-dimensional slot burner and cylidrical-shaped burners, respectively. Huang and Lin (1994) studied the flame behavior and the time-averaged thermal structure for various C_3H_8 and air flows. Schefer et al. (1987) and Namazian et al. (1989) performed velocity and concentration measurements using laser Doppler velocimetry and a combined Raman scattering and laser-induced fluorescence imaging in turbulent flow for CH_4. Lee and Onuma (1991) also measured velocity, temperature and chemical species in turbulent flow for H_2 in order to compare with numerical simulation of a k-ε model.

Although they emphasized the importance of vortical structures in bluff-body burners, the relationship between the vortical and thermal structures under unsteady vortical motion has not been understood fully in the experimental studies. While, more recently, direct numerical simulations have been performed in the transitional flow regime for jet diffusion flames to capture the temporal and spatial development of vortical and thermal structures, i.e., Katta and Roquemore (1993), Yamashita et al. (1996). Such a simulation will be extended to bluff-body burners in the near future. However, there have been few studies providing time-dependent experimental data to test and refine mathematical modeling. These apects have motivated the present investigation. Vortical

and thermal structures in a bluff-body burner are studied experimentally in the transition from laminar to turbulent flow as a necessary initial step in a more realistic situation involoving fully turbulent flow. Because we focus attention on the effect of annular air flow on the flame, and it is expected that the fuel jet in the transition regime is responsive to the annular air flow.

2. Experimental Apparatus and Procedure

The bluff-body, vertical, unducted combustor used here consisted of a fuel nozzle located concentric to an annular region where air flowed, as shown in Fig. 1. Commercial-grade propane was employed as the fuel gas. The diameters of the fuel nozzle D_j, the inner annulus D_i and the outer annulus D_o were 10 mm, 42 mm and 56 mm, respectively. One of the objectives of the present study is to examine the effect of the annular air velocity. The test matrix consisted of measurements over a range of annular air velocity under a fixed fuel velocity, listed in Table 1. It should be noted that the jet at this fuel velocity belongs to the transition regime, in the absence of the annular air flow.

Table 1. Experimental conditions.

	central fuel jet		annular air flow.		
case	u_j(m/s)	Re_j	u_a(m/s)	Re_a	u_a/u_j
A	0.84	1957	0.0	0.0	0.0
B	0.84	1957	0.62	563	0.74
C	0.84	1957	1.84	1632	2.19

The relationship between vortical and thermal structures was examined by flow visualizations and temperature measurements. A schematic diagram of the experimental set-up is shown in Fig. 2. The vortical structure was visualized by combination of the shadowgraph method and 16 mm high-speed cinematography. A projector lamp was the continuous light source. The motion pictures were analyzed with an image processor.

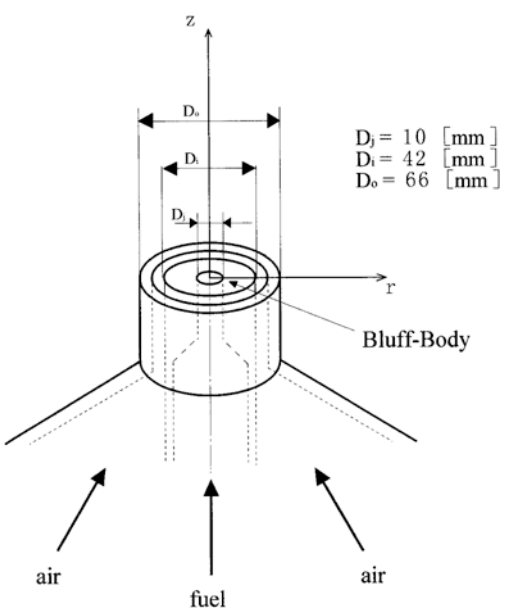

Fig. 1. Bluff-body burner.

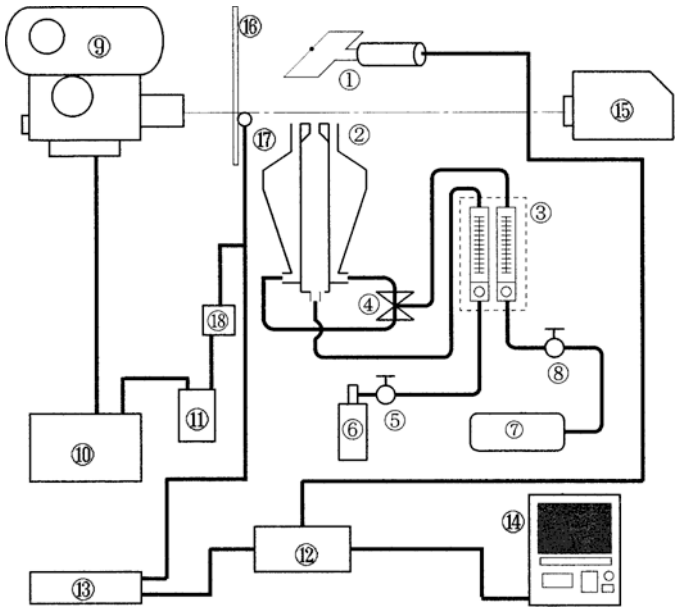

q Thermocouple
w Bluff-body combustor
e Rotameters
r Two ways valve
t Reduced pressure adjustor
y Propane gas vessel
u Air compressor
i Air transformer
o 16mm High-speed camera
!0 High-speed camera control panel
!1 Trigger voltage generator
!2 Compensation circuit
!3 A/D converter
!4 Oscilloscope
!5 Slide projector
!6 Frosted glass
!7 Light-emitting diode
!8 Buffer

Fig. 2. Experimental apparatus.

A fine wire thermocouple compensated for the effects of thermal inertia was employed to examine the characteristics of temperature fluctuations, i.e., Pt-Pt/Rh 13 %, 50 μm in diameter. No coatings were applied to the thermocouple to inhibit catalytic activity because of the increase in the time constant. The thermocouple with the compensator is presumed to follow temperature fluctuations of 2 kHz. The dominant temperature fluctuation is less than 0.5 kHz in this experiment. The output of the compensated thermocouple was digitized by a 12 bit analogue-to-digital converter for 16384 data points. The information on the flow visualization and temperature measurement was simultaneously monitored to make clear the interrelation of these data.

3. Results and Discussion

3.1 Vortical Structure

In the bluff-body combustor, a recirculation zone is established at the burner exit, as a result of the expansion of the annular air flow. Figure 3 shows a representative photograph of vortical structures inside the flame by the Mie-scattering laser sheet lighting technique (Nishimura et al., 1993). The visible flame is yellow and the green is Mie scattered laser light from the soot particles produced in the fuel flow due to thermal decomposition. Two toroidal vortices exist stably in the recirculation zone, in contrast to non-combusting flow. When we aim at a small vortex near the central fuel jet in the recirculation zone, it is expected from the photograph that this vortex plays an important role on the shear layer instability of the fuel jet. The recirculation zone depends on the fuel and air flows, and also the flame position on the bluff-body surface markedly changes. Figure 4 shows the time-averaged maximum temperature locations representing flame shapes for three different conditions, i.e., cases A, B and C shown in Table 1. The dotted line denotes 90% of the maximum temperature. The flame position at the burner exit shifts from the inner circle of the bluff-body surface to the outer circle, in the presence of annular air flow. There exists no recirculation zone for zero annular air flow (see case A), but the recirculation zone is formed by the presence of air flow and expands in the axial direction with increasing the air velocity (see cases B and C).

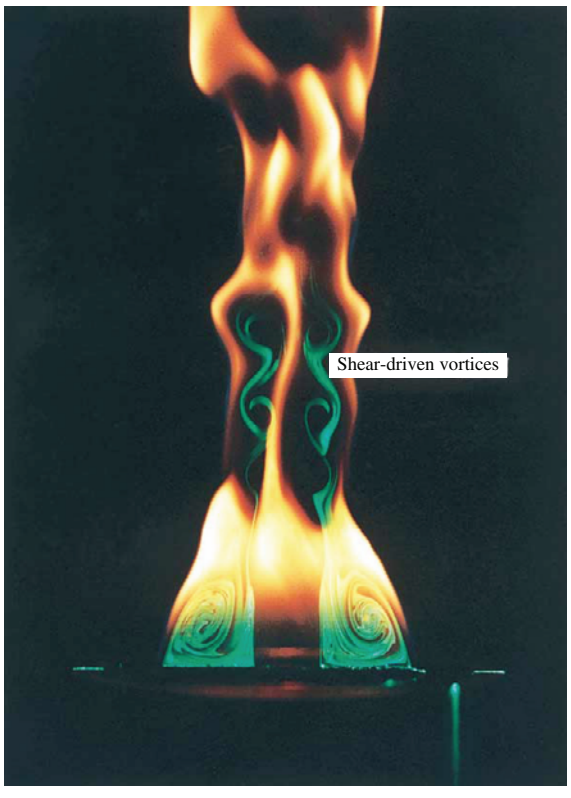

U_a=123.7cm/s(Re_a=1154), U_j=106.1cm/s(Re_j=2427)

Fig. 3. Flow visualization by laser sheet ligting technique.

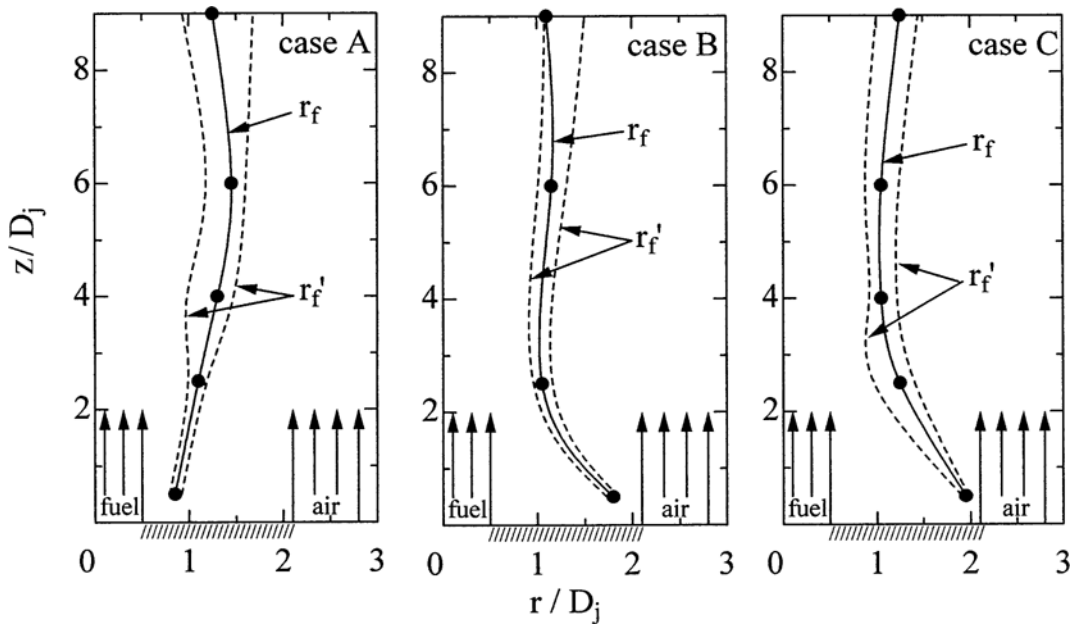

Fig. 4. Flame shapes for cases A, B and C.

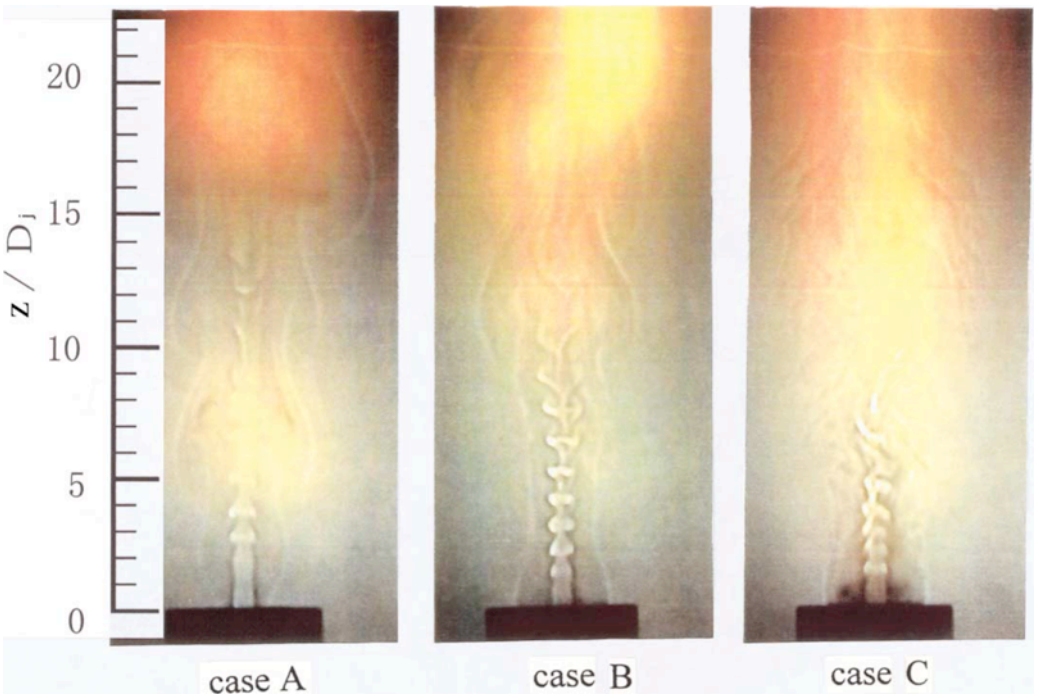

Fig. 5. Shadowgraphs for cases A, B and C.

Figure 5 shows the shadowgraph images which are arranged to correspond to the flame positions of Fig. 4. In contrast to the Mie-scattering laser sheet lighting technique, the shadowgraph images do not show the detailed vortical structures in the recirculation zone. While the vortical structures of the central fuel jet and annular air flow and the mixing characteristics are observable. Case A shows a double-vortex structure with self-sustained oscillation, i.e., small-scale inner and large-scale outer vortices separated by the flame. The formation of inner vortices is due to the shear layer instability of the fuel jet inside the flame and the vortex development is weak near the burner exit, because the fuel Reynolds number is low. While the outer vortices are driven by thermal buoyancy due to heat release. The dynamic vortical structures are very simular to the previous result of a single jet diffusion flame with no bluff-body by Davis et al. (1991). Cases B and C indicate the effect of annular air flow.

In particular, for case C, the outer vortices are not clearly discernible in the shadowgraph, but the inner vortices become more clear, which supports the expectation based on the flow visualization image in Fig. 3. That is, the small vortex in the recirculation zone exerts a strong shear effect on the surface of the central fuel jet. Furthermore, an interesting phenomenon is the fact that the direction of rotation of the inner vortices changes downstream and its location tends to move slightly upstream with an increase of the annular air velocity. The reversal phenomenon of the inner vortices has been known in single jet diffusion flames for propane fuel (Eickhoff et al., 1985; Katta and Roquemore, 1993). However, this phenomenon is found to vary significantly with the annular air velocity in the present study.

Figure 6 presents sample plots of the trajectories of the inner vortices in the near nozzle region for Cases B and C. Similar analysis of vortex and flame dynamics by high speed visual observations has been performed in the near-field and far-field for jet diffusion flames, respectively (Savas and Gollahalli, 1986; Mungal et al., 1991; Newbold et al., 1997). The trajectories were obtained from motion pictures made at 1000 frames/s. Numerous interesting features are included in these diagrams. For case B, a comparison of combusting and non- combusting flows indicates that the presence of the flame keeps a long coherence length of inner vortices. The ratio of the convection velocity to the exit fuel velocity c/U_j is 0.92 and 0.70 in combusting and non-combusting flow,

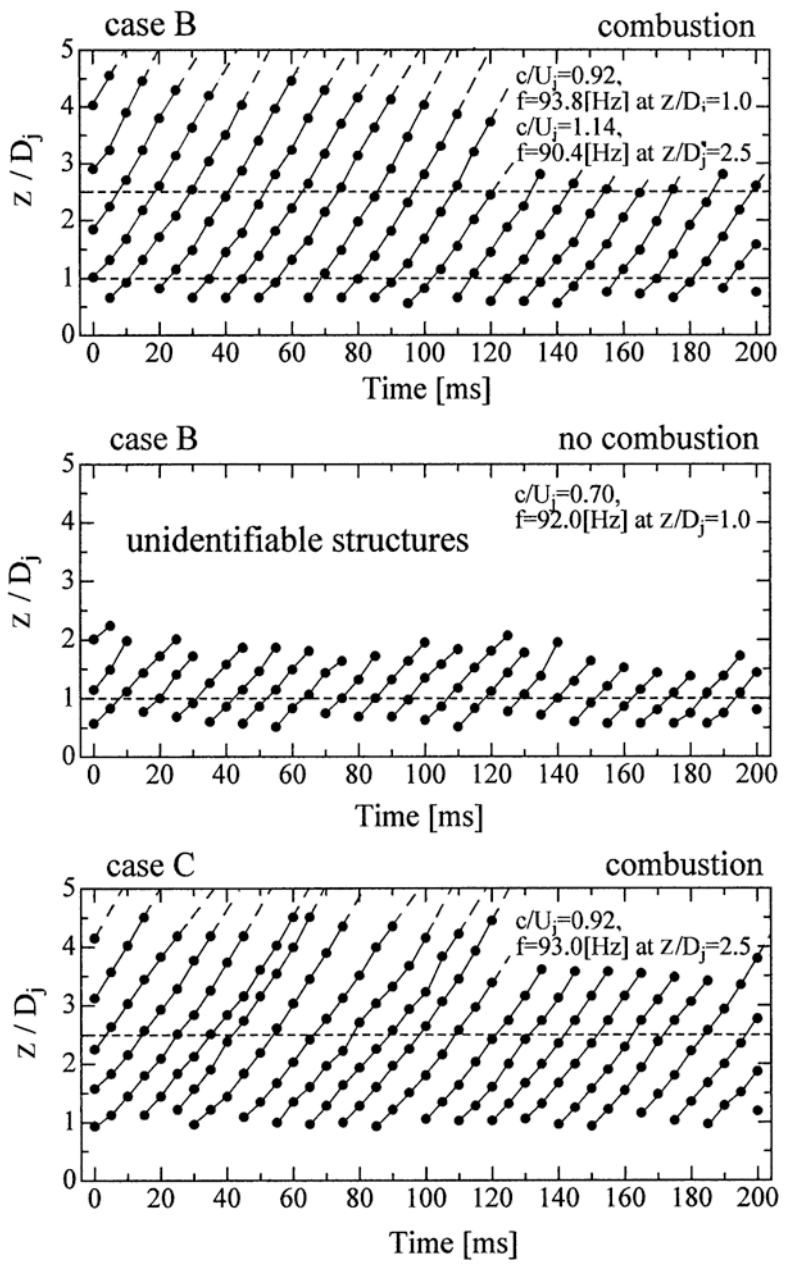

Fig. 6. Trajectories of inner vortices.

respectively at the axial position of 1 diameter from the nozzle exit i.e., z/D_j=1.0. Its value for combustion exceeds unity further downstream. This means that the convection velocity is accelerated due to thermal expansion of hot gases in the flame. While the passing frequencies in both flows do not change siginificantly at $z/D_j = 1$, and thus the spacing of vortices becomes larger in the presence of the flame. The convection velocity for case C is smaller than that for case B at $z/D_j = 2.5$, but the passing frequencies are close. The reduction of the convection velocity probably promote earier breakdown of inner vortices as shown in Fig. 5. In the present study, the Strouhal number for the passing frequency of the inner vortices (fD_j/U_j) is in the range of 1.07 - 1.09 at $Re_j = 1957$. This is out the range $0.24 < St_j < 0.5$ in which the preferred frequency mode is known to lie for uniform density jets. The effect of the fuel velocity excluded from the scope of the present study will be subject of future investigations.

Thus, it is concluded that the annular air flow has a great influence on the dynamic vortical structures of the central fuel jet through the flame in the bluff-body burner.

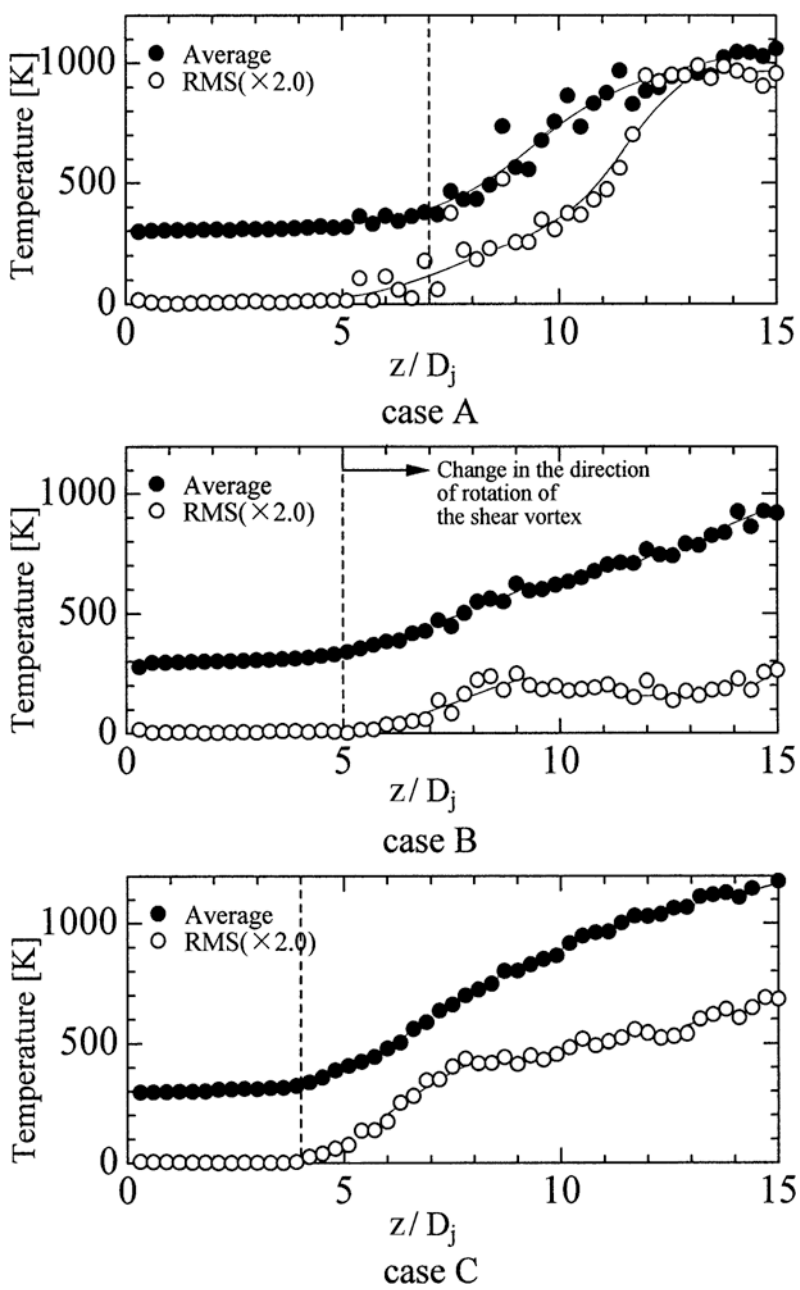

Fig. 7. Time-averaged and rms temperature distiributions along the axial line of the burner.

3.3 Thermal Structure

The thermal structure is complicated and dominated by the vortical structures mentioned above. Figure 7 shows the time-averaged and rms temperature distributions along the axial line of the burner for cases A, B and C. In all cases, the time-averaged and rms values increase with the axial distance, and the steep gradient of the time-averaged temperature corresponds to that of the rms temperature. The change in rotation of the inner vortices as shown in Fig. 5 appears to have an impact on the thermal structure. It is also striking that the rms temperature at a downstream location of z/D_j = 1.5 for case A is significantly larger than that for case C, while its temperature for case B is smaller.

Figure 8 shows the radial profiles of the time-averaged temperature at three specified axial positions, i.e., z/D_j = 2.5, 6.0 and 9.0. In all cases, the peak temperature decreases with the axial distance. The temperature reduction for cases A and C is larger than that for case B, and their radial profiles broaden downstream. These results suggest strong interactions with the dynamic vortical structures mentioned above.

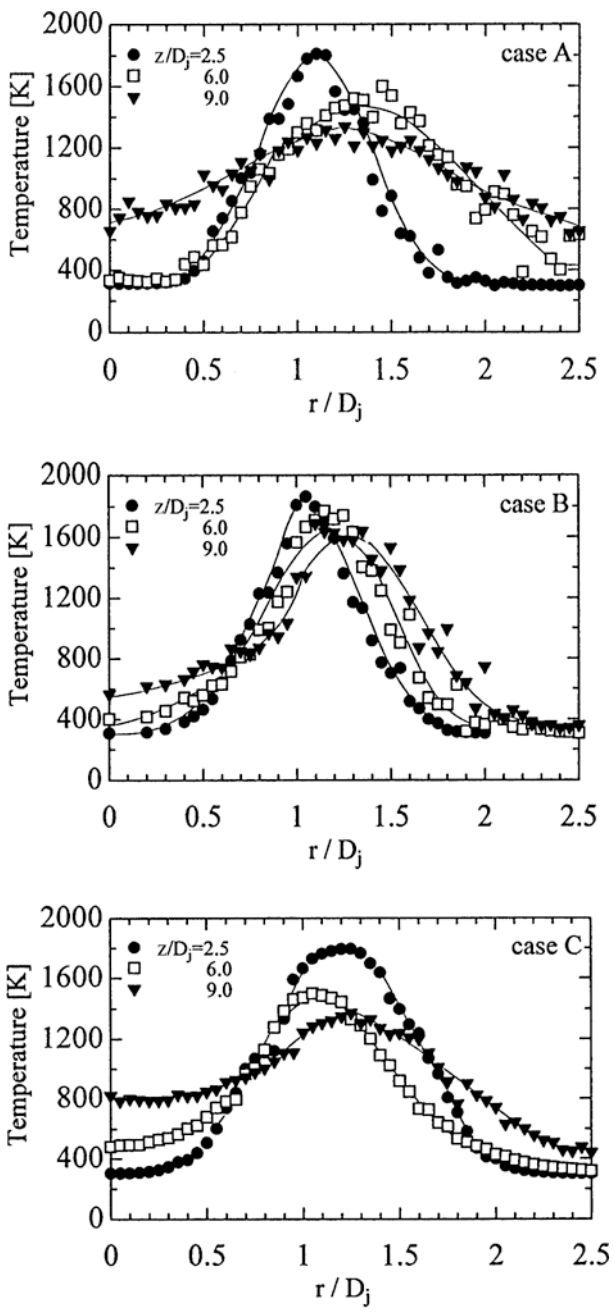

Fig. 8. Radial profiles of time-averaged temperature.

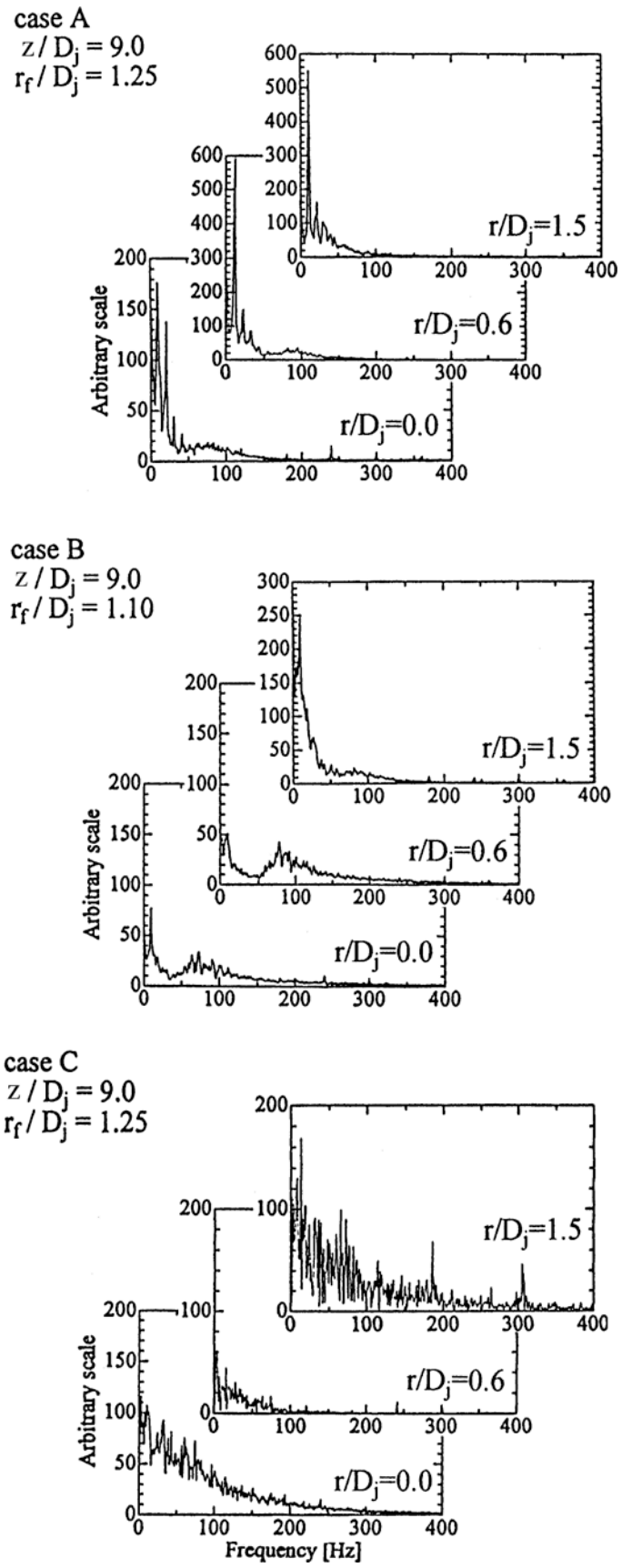

Fig. 9. Frequency spectrum of temperature at specified locations.

Although the time-averaged and rms temperatures indicate global features of the thermal structure through the flame, more precise information can be retrieved from the frequency spectrum and probability density function of the temperatures. Only a few examples at specified locations are shown here.

Figures 9 and 10 display the frequency spectrum and probability density function at an axial downstream location of $z/D_j = 9.0$ and radial locations of $r/D_j = 0.0$, 0.6 and 1.5, respectively. For case A, outside the flame ($r/D_j = 1.5$), a single-predominant low frequency of 10 Hz is induced by the outer vortices and its harmonics are observed. While inside the flame, a weak predominant frequency of 93 Hz induced by the inner vortices appears, in addition to low frequencies by the outer vortices (see the results at $r/D_j = 0.0$ and 0.6). Similar trends are observed for case B, but higher harmonics by the outer vortices disappear and there are two predominant frequencies inside the flame. That is, the high frequency component is comparable to the low frequency one, indicating only a weak interaction between the inner and outer vortices. However, for case C, there is no predominant frequencies at a downstream location $z/D_j = 9.0$ in all radial positions, suggesting the presence of turbulent eddies due to a higher annular air velocity. Outside the flame, the probability density functions in all cases vary over a wide range from the room temperature to the flame temperature. This is related to radial movement of the flame due to the vortices. However, inside the flame, the extent of the temperature variation strongly depends on the value of annular air velocity. In particular the extent for case B is small at $r/D_j = 0.0$.

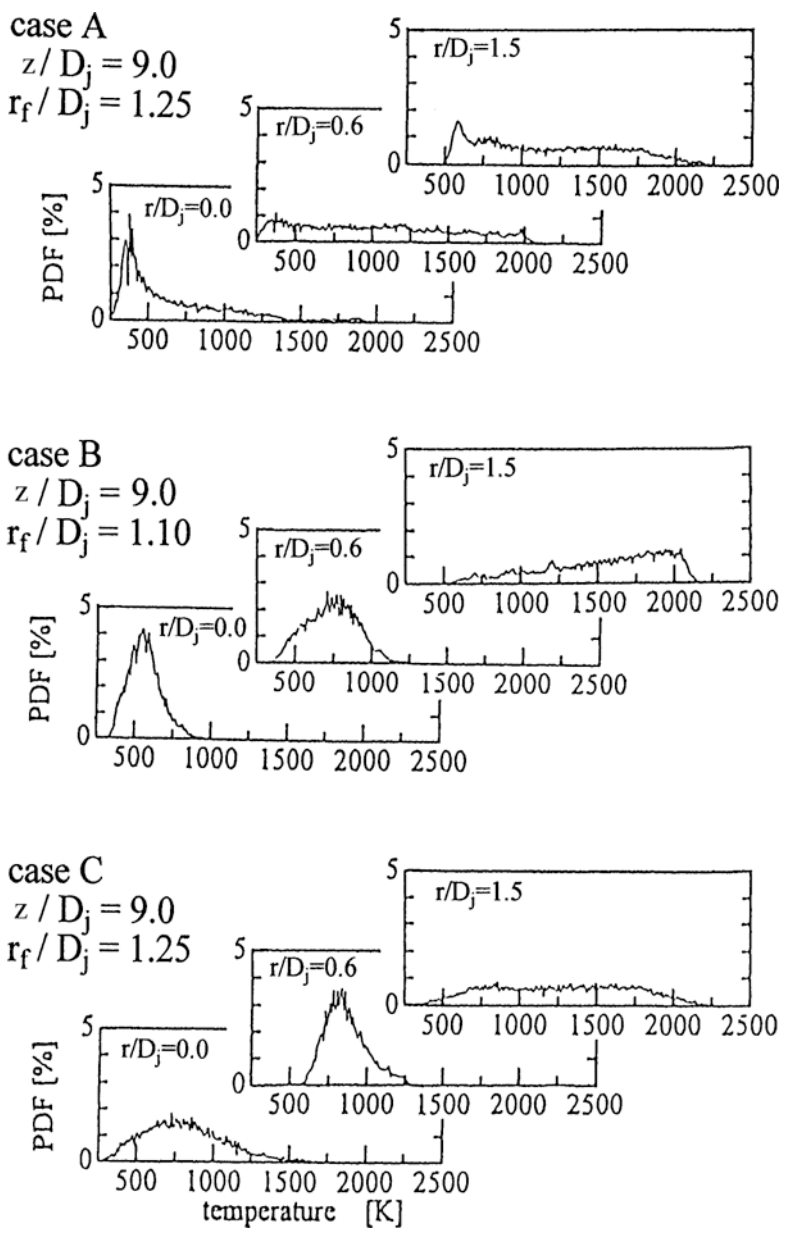

Fig. 10. Probability density function of temperature at specified locations.

Figure 11 shows contour lines of constant rms temperature normalized by their time-averaged values for cases A, B and C. They exhibit a clear feature of temperature fluctuation in the near-field of the burner, depending on the annular air flow. That is, the large-scale outer vortices due to thermal buoyancy and the small-scale eddies induced by the annular air flow dominate the dynamic thermal field rather than the inner vortices due to jet instabilities for cases A and C, respectively, in consideration of the frequency spectrum and probability density function as shown in Figs. 9 and 10. While, for case B, the interaction between the inner and outer vortices is rather weak, which is also supported from the results of Figs. 7 and 8. Each set of vortices independently act on the thermal field inside and outside the flame, respectively.

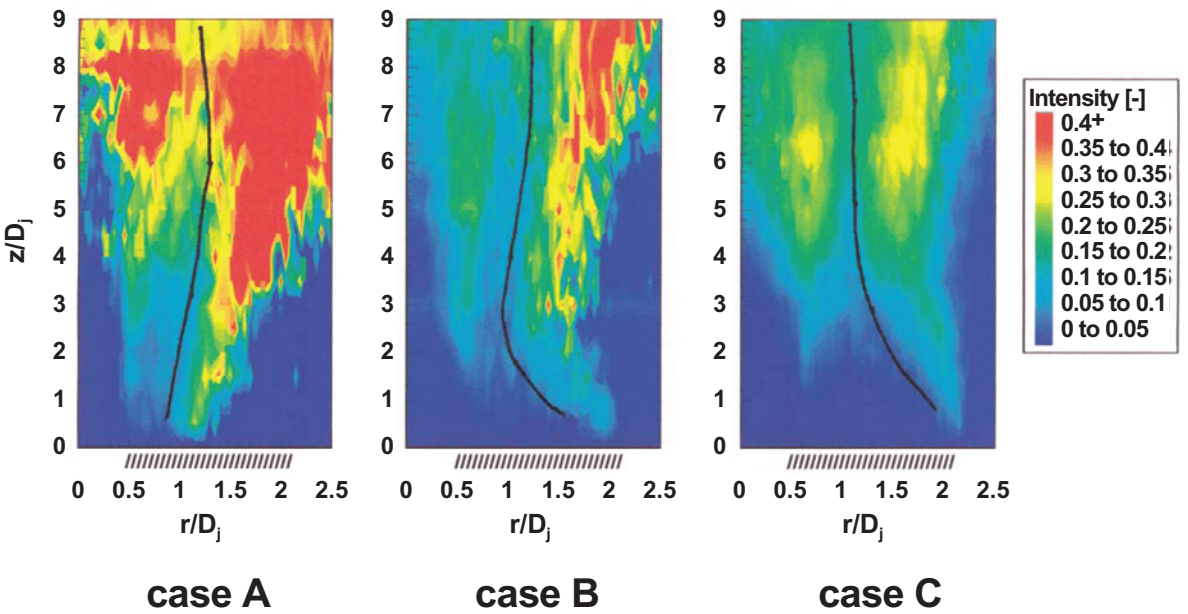

Fig. 11. Contour lines of rms temperatures normalized by their time-averaged values.

4. Conclusions

We studied experimentally the relationship between the vortical and thermal structures in non-premixed propane flame for a bluff-body burner in the transition from laminar to turbulent flow. The information on the flow visualization and temperature measurement is simultaneously monitored. Although there are interactions between two vortices inside and outside the flame, the annular air flow has a stronger impact on the flame, rather than the central fuel jet in this experimental range.

References

Chin, L.P. and Tankin, R. S., Vortical Structures in a 2-d Vertical Bluff-body Burner, Combust. Sci. and Tech., 80 (1991), 207-229.

Davis, R. S., More, E. F., Roquemore, W. M., Chen, L. D., Vilimpoc, V. and Gross, L. P., Preliminary Results of a Numerical-exp erimental Study of the Dynamic Structure of a Buoyant Jet Diffusion Flame, Combust. Flame, 83 (1991), 263-270.

Eickhoff, H. and Winandy, A., Visualization of Vortex Formation in Jet Diffusion Flame, Combust. Flame, 83 (1991), 263-270.

Hung, R. F. and Lin, C. L., Characteristic Modes and Thermal Structures of Non-premixed Circular-disc Stablized Flames,Combust. Sci. and Tech., 100 (1994) 123-139.

Katta, V. R. and Roquemore, W. M., Role of Inner and Outer Structures in Transional Jet Diffusion Flame, Combust. Flame, 92 (1993), 274-282.

Lee, C. E. and Onuma, Y., Experimental Study of Turbulent Diffusion Flames Stabilized on a Bluff Body-1st Report, Flame Structu re, Trans JSME Ser. B, 57 (1991), 4266-4271.

Li, X. and Tankin, R. S., A Study of Cold and Combusting Flow around Bluff-body Combustors, Combust. Sci. and Tech., 52 (1987), 173-206.

Mungal, M. G., Karasso and Lozano, A., The Visible Structure Jet Diffusion Flames: Large-scale Organization and Flame Tip Oscil lation, Combust. Sci. and Tech., 76 (1991), 165-185.

Namazian, M., Kelly, J., Schefer, R. W., Johnston, S. C. and Long, M. B., Non-premixied Bluff-body Burner Flow and Flame Imagin g Study, Exp. Fluids, 8 (1989), 216-228.

Nishimura, T. and Takemori, I., Vortical Structures of Combusting Flow around Bluff-body Burners, Proc. 7th Int. Symp. on Flow Visualization 1995 (Seattle), (1995), 512-517.

Nishimura, T., Ota, M. and Kojima, N., Vortex Structure of Combusting Flow around a Bluff-body Combustor, Album of Visualizatio n, The Visualization Society of Japan, 10, (1993), 7-8.

Newbold, G. J. R., Nathan, G. J. and Luxton R. E., Large-scale Dynamics of an Unconfined Precessing Jet Flame, Combust. Sci. an d Tech., 126,

(1997), 71-95.
Roquemore, W. M., Tankin, R. S., Chiu, H. H. and Lottes, S. A., A Study of a Bluff-body Combusting using Laser Sheet Lighting, Exp. Fluids, 4 (1986), 205-213.
Savas, O. and Gollahalli, S. R., Flow Structure in Near-nozzle Region of Gas Jet Flames, AIAA J., 24, (1986), 1137-1140.
Schefer, R. W., Namazian, M. and Kelly, J., Velocity Measurements in a Turbulent Non-premixed Bluff-body Stabilized Flame, Comb ust. Sci. and Tech., 56 (1987), 101-138.
Yamashita, H., Idota, T. and Takeno, T., Effect of Fuel on Transition of Fuel Jet Diffusion Flame, Trans JSME Ser. B, 62 (1996), 1226-1233.

Authors' Profiles

Tatsuo Nishimura: He is a professor of mechanical engineering at Yamaguchi University. He recieved a B.E. (1974) in chemical engineering from Yamaguchi University, an M.E. (1976) in chemical engineering from Toyama University and a Ph.D. (1981) in chemical engineering from Hiroshima University. He has published extensively in the areas of heat, mass and momentum transfer such as enhanced heat and mass transfer, solidification of multi-component systems, double-diffusive convection and non-premixed combustion.

Takeshi Kaga: He is a customer engineer at Hewllett Packard Japan Ltd. in Tokyo. He holds B.E. (1995) and M.E. (1997) in mechanical engineering from Yamaguchi University. He is a member of JSME.

Kazuyuki Shirotani: He is a consulting engineer at Kyudenko Corporation in Fukuoka, Japan. He recieved his undergruaduate degree (1997) in mechanical engineering from Yamaguchi University.

Junya Kadowaki: He is an engineer at Izumo Murata Manufacturing Company in Hikawa, Japan. He holds B.E. (1996) and M.E. (1998) in mechanical engineering from Yamaguchi University.